The influence of metabolic network structures and energy requirements on xanthan gum yields

Fabien Letisse, Paule Chevallereau, Jean-Luc Simon, Nic Lindley

ELSEVIER

Journal of Biotechnology 99 (2002) 307–317

JOURNAL OF Biotechnology

www.elsevier.com/locate/jbiotec

The influence of metabolic network structures and energy requirements on xanthan gum yields

Fabien Letisse [a,b], Paule Chevallereau [b], Jean-Luc Simon [b], Nic Lindley [a,*]

[a] *Laboratoire de Biotechnologie-Bioprocédés, UMR INSA/CNRS, Centre de Bioingenierie Gilbert Durand, INSA, 135 Avenue de Rangeuil, 31077 Toulouse cedex 4, France*

[b] *Laboratoires des Recherches Techniques, Rhodia Food, B.P. 30, 79500 Melle, France*

Received 11 July 2001; received in revised form 21 May 2002; accepted 24 May 2002

Abstract

The metabolic network of *Xanthomonas campestris* is complex since a number of cyclic pathways are present making simple stoichiometric yield predictions difficult. The influence of certain pathway configurations and the resulting variations in flux have been examined as regards the maximum yield potential of this bacteria for xanthan gum production. These predictions have been compared with experimental results showing that the strain employed is functioning close to its theoretical maximum as regards yield criteria. The major constraint imposed on the network concerns energy availability which has a more pronounced effect on yield than carbon precursor supply. This can be attributed to the relatively high maintenance requirements determined experimentally and incorporated into the model. While some of this overall energy burden will undoubtedly be associated with incompressible metabolic requirements such as sugar uptake and xanthan efflux mechanisms, future strain improvement strategies will need to attack other non-essential energy-consuming reactions, if yields are to be further increased.

Keywords: *Xanthomonas campestris*; Flux modelling; Metabolic engineering; Bioenergetics

1. Introduction

Industrial production of xanthan gum using *Xanthomonas campestris* has improved over several decades due to both genetic selection and empirical process improvements. To date, pragmatic engineering of this organism's metabolic network has not been widely employed other than as a means to modify organic acid composition of the polysaccharide. This is due largely to a restricted understanding of the metabolic constraints governing carbon and energy flux within the central pathways.

The pathways of central metabolism in *X. campestris* closely resemble those described for *Pseudomonas aeruginosa* (Temple et al., 1998), in which two discrete system exist for the oxidative metabolism of glucose: the periplasmic direct oxidative pathway involving glucose dehydrogenase activity; and the intracellular phosphorylative pathway (Whitfield et al., 1982). Both pathways

* Corresponding author

0168-1656/02/$ - see front matter
PII: S0168-1656(02)00221-3

lead to the production of 6-phosphogluconate (6PG), which may be further metabolised via the Entner–Doudoroff pathway, with the pentose–phosphate pathway fulfilling a minor role for anabolic precursor requirements in *Xanthomonas* species (Zagallo and Wang, 1967). Furthermore, glyceraldehyde-3-phosphate (GAP) can either enter glycolysis or be recycled through the central cycle (Hochster and Katznelson, 1958). To date, the distribution of the carbon flux through such a central metabolic network has not been established during xanthan gum production. Theoretical studies of the energy requirements for xanthan synthesis (Jarman and Pace, 1984) have indicated that the proportion of energy derived from the oxidation of the carbon substrate (glucose), either completely to CO_2 or partially to various oxidized products, which may be integral components of the xanthan pattern, is strongly dependent on the xanthan composition and on the ATP/O ratio. Despite this, the influence of carbon distribution through the various possible metabolic network configuration on rates of production and yield of xanthan gum has not been evaluated.

Industrial production of xanthan gum is generally achieved throughout batch cultivation using non-limiting glucose or glucose derivates such as starch hydrolysates as carbon feedstock. In this paper, the metabolic constraints specific to each of the central pathways involved in glucose metabolism have been established and the effect of hypothetical carbon flux distribution on product yields calculated. These data are compared with fermentation data concerning xanthan gum production.

2. Materials and methods

2.1. Microorganism and cultivation procedures

The strain used throughout this work was *X. campestris* ATCC 13951. Culture procedures were those described by Letisse et al. (2001) except that glucose was the carbon substrate. Growth and production was followed using a 20 l bioreactor (Biolafitte) equipped with wide diameter stirring paddles (13 cm). The growth medium consisted of glucose (42 g l^{-1}), NH_4NO_3 (1.125 g l^{-1}), $(NH_4)_2HPO_4$ (0.217 g l^{-1}), $MgSO_4 \cdot 7H_2O$ (0.25 g l^{-1}) and soybean flour hydrolysate (15 ml l^{-1}). The pH was maintained at 7.0 throughout the fermentation by automatic addition of NaOH (2 M), the temperature was regulated at 28 °C and stirrer speed increased as the culture progressed to maintain dissolved oxygen concentrations superior to 20% saturation. Inocula were prepared in overnight shake flask cultivation using a chemically defined medium with increased buffering capacity containing glucose (42 g l^{-1}); K_2HPO_4 (5 g l^{-1}); NH_4Cl (1.94 g l^{-1}); $MgSO_4 \cdot 7H_2O$ (0.25 g l^{-1}); $CaCl_2 \cdot 2H_2O$ (0.018 g l^{-1}); $ZnSO_4$ (0.012 g l^{-1}); $FeCl_3 \cdot 6H_2O$ (0.0024 g l^{-1}); H_3Bo_3 (0.006 g l^{-1}) and citric acid (2 g l^{-1}).

2.2. Analytical methods

Fermentation samples were chilled on ice and centrifuged immediately (30 min at $33\,000 \times g$ at 4 °C) to separate cells from the liquid phase. When necessary samples were diluted in KCl (1% w/v) to decrease sample viscosity thereby avoiding incomplete separation of cells from the broth. Cell free supernatant was removed and stored at −15 °C for further analysis. Cell biomass was washed in KCl solution (0.2% w/v), centrifuged for 10 min at $9000 \times g$ at 4 °C in previously weighed centrifugation tubes, washed in situ with distilled water and dried to constant weight at 60 °C under partial vacuum. The difference in tube weight was used to calculate the cell dry weight concentration by relating this value to the initial sample volume. These samples were also used for elemental analysis to determine the carbon, hydrogen, oxygen and nitrogen content of the biomass (Ecole de Chimie, Toulouse). Biomass was also followed by direct absorbance measurements at 600 nm against a medium blank.

Xanthan gum in the centrifugation supernatant was precipitated using isopropanol and the precipitate dissolved in KCl solution (0.2% w/v), reprecipitated in isopropanol and dried to constant weight at 60 °C under partial vacuum to determine the xanthan concentration. The xanthan was then hydrolysed in HCl (1 M) at 110 °C for 1 h. The chemical composition of the hydrolysed

xanthan (glucose, mannose, glucuronate, pyruvate and acetate content) was determined by HPLC using an HPX87H column (Biorad) maintained at 48 °C with H_2SO_4 (5 mM) as eluant. Detection was by UV and refractometric detectors placed in series at the column outlet.

After xanthan precipitation, the remaining aqueous phase sample was used to detect the residual glucose concentration using the same HPLC procedure except that the eluant was H_2SO_4 (8.5 mM) and the column temperature was 24 °C. The nitrate concentration within this same sample was determined by HPLC analysis using an Aquapore RP-300 column (Brownlee Labs) at 24 °C with octylamine solution (0.01 M, adjusted to pH 4 with H_3PO_4) as eluant. Peak detection was by UV analysis at 210 nm wavelength. The ammonium concentration was determined in the supernatant using an ammonia specific electrode (Orion 95-12) while the phosphate concentration was determined by the ascorbic acid method.

Rates of gas influx and efflux were measured by a volumetric counter and the gas outlet was analysed periodically throughout the fermentation by gas chromatography (Loubiere et al., 1992).

2.3. Enzyme activity measurements

Cells were harvested by centrifugation (30 000 × *g* for 25 min at 4 °C) and washed twice with Tris–HCl buffer (100 mM, pH 7.5) before resuspending in Tris-tricarballylate buffer (40 mM Tris + 10 mM tricarballylate, pH 7.8) containing $MgCl_2$ (5 mM) and glycerol (20% v/v). Cells were disrupted by ultrasonic treatment as previously described (Dominguez et al., 1998). Protein concentration of the enzyme extracts was determined by the Lowry method using bovine serum albumin as standard protein solution.

The specific activity of GAP dehydrogenase was assayed as described previously (Dominguez et al., 1998) while fructose bisphosphatase and fructose bisphosphate aldolase activities were assayed using the methods described by Conrad and Schlegel (1977) except that the assay pH was 7.8.

2.4. Flux balance model

A metabolic network has been established for the calculation of intracellular fluxes (Fig. 1) based on the established biochemistry of central metabolism as described in the scientific literature (Hochster and Katznelson, 1958; Zagallo and Wang, 1967; Whitfield et al., 1982), the biosynthetic pathway to xanthan gum as described by Becker et al. (1998), and metabolite requirements for biomass biosynthesis as determined for *Ralstonia eutropha* by Ampe et al. (1997): see Table 1. Experimental kinetic data which were used to calculate the specific rates (substrate consumption rates and growth rates) and the maintenance coefficient which were used as inputs for the model. Outputs towards biomass were determined by multiplication of the anabolic demand by the specific growth rate. The carbon flux at each step of the pathway was determined for each biochemical reaction assuming that metabolite pools undergo variations in concentrations which may be considered insignificant in comparison to the flux. The maximal yield of xanthan gum was calculated as a function of an imposed carbon flux distribution at selected metabolic nodes. The flux repartition through the various pathways of the metabolic network was then established in order to meet the energetic supply-and-demand balance. The calculations to maximise xanthan gum yield were performed using the EXEL V solver (Microsoft) for different energetic efficiencies of the respiratory chain, depending on the number of proton translocation sites.

3. Results and discussion

3.1. Determination of maintenance coefficient

If energy demand associated with cell growth can be estimated from existing knowledge of the anabolic pathways and macromolecule assembly mechanisms, a significant part of the microorganism's energetic budget is often used for non-identified energy requiring processes. This is frequently covered by the maintenance coefficient which can be quantified by analysis of growth

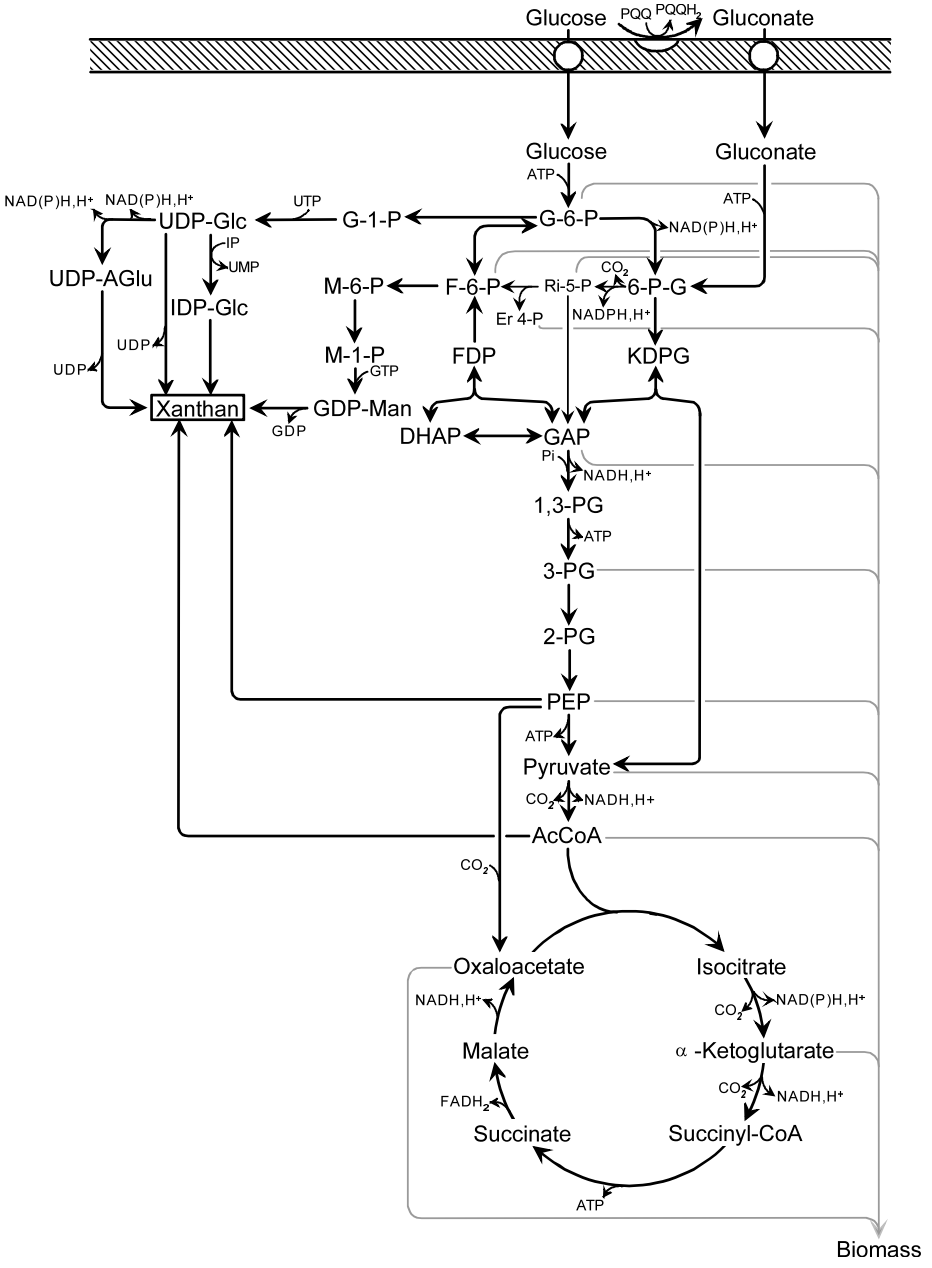

Fig. 1. Metabolic network considered. Abbreviations: G-6-P, glucose-6-phosphate; F-6-P, fructose-6-phosphate; FDP, fructose-1,6-bisphosphate; DHAP, dihydroxyacetone-phosphate; GAP, glyceraldehyde-3-phosphate; 6-P-G, 6-phosphogluconate; KDPG, 2-keto-3-deoxy-6-phosphogluconate; 1,3-PG, 1,3-diphosphoglycerate; 3-PG, 3-phosphoglycerate; 2-PG, 2-phosphoglycerate; PEP, phosphoenolpyruvate; AcCoA, acetyl coenzyme A; Ri-5-P, ribose-5-phosphate; Er-4-P, erythrose-4-phosphate; G-1-P, glucose-1-phosphate; M-6-P, mannose-6-phosphate; M-1-P, mannose-1-phosphate; UDP-Glc, UDP-glucose; UDP-AGlu, UDP-gluconate; GDP-Man, GDP-mannose; IP, isoprenoid phosphate; IDP, isoprenoid pyrophosphate.

Table 1
Intermediate metabolites and energy requirements for the formation of 1 g of biomass of the bacterium *R. eutropha* during exponential growth (Ampe et al., 1997)

Precursor metabolite	Amount required (mmol g^{-1} cells)
Glucose-6P	0.36
Fructose-6P	0.10
Pentose-5P	0.52
Erythrose-4P	0.34
Triose-P	0.09
3-Phosphoglycerate	1.40
Phosphoenolpyruvate	0.66
Pyruvate	2.60
Acetyl-CoA	2.52
α-Ketoglutarate	1.62
Oxaloacetate	1.58
ATP	40.8
$NADPH,H^+$	18.3
$NADH,H^+$	−2.9

kinetics. In this study, the maintenance coefficient were estimated using experimental data from batch cultivation on glucose (Fig. 2). This batch cultivation was characterised by diminished specific rates throughout the fermentation as xanthan accumulates. Specific rates of both glucose consumption (q_{glc} as mmol glucose g^{-1} cells h^{-1}) and xanthan production (υ_{xth} as mmol pentasaccharide unit g^{-1} cells h^{-1}) obey linear relationships with regard to the specific growth rate (μ) as summarised by the following equations:

$$q_{glc} = 20.2\mu + 1.02$$

$$\upsilon_{xth} = 1.68\mu + 0.12$$

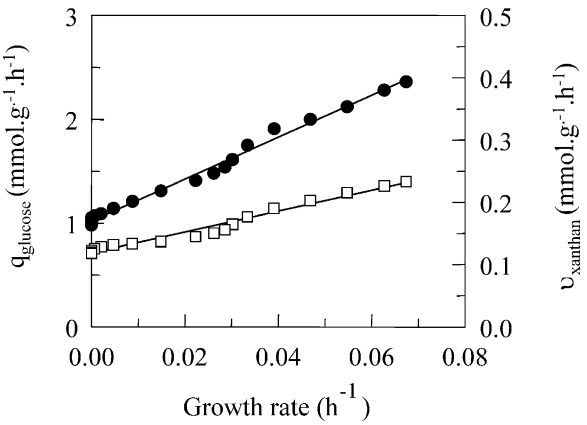

Fig. 2. Relationships between specific rates of glucose consumption ($q_{glucose}$, ●) and xanthan production ($\upsilon_{xanthan}$, □) and the specific growth rate during batch cultivation of *X. campestris* on glucose.

The following general equation was used for the calculation of the maintenance coefficient:

$$q_{glc} = \frac{\mu}{Y_x} + \frac{\upsilon_{xth}}{Y_{xth}} + m \quad (1)$$

where q_{glc} is the specific rate of glucose consumption, μ is the specific growth rate, Y_x is the growth yield, υ_{xth} is the specific rate of xanthan production, Y_{xth} is the xanthan yield and m is the maintenance coefficient. This equation can be written as follows:

$$q_{glc} = \left(\frac{Y_{xth} + 1.68\,Y_x}{Y_{xth}\,Y_x}\right)\mu + \frac{0.12}{Y_{xth}} + m \quad (2)$$

The experimental value for the maintenance coefficient, which can be expressed as a part of the substrate consumption rate was estimated at $\mu = 0$, taking into account the energetic requirement for xanthan biosynthesis. The following stoichiometric relationship can be used with respect to the production and the polymerisation of 1 U of xanthan including 0.5 mol of pyruvate and 1 mol of acetate:

$$5.75\text{Glucose} + 10.75\text{ATP} \rightarrow [C_{33.5}H_{51}O_{28}] + 1CO_2 + 4.5\text{NAD(P)}H_2 \quad (3)$$

An estimated maintenance coefficient of 0.33 mmol g^{-1} h^{-1} was calculated. A similar maintenance coefficient value (0.365 mmol g^{-1} h^{-1}) was calculated by the method of Jarman and Pace (1984) for a strain of *X. campestris*, cultivated in a sulphur-limited continuous culture, using glucose as carbon source.

3.2. Metabolic network of *Xanthomonas campestris*

3.2.1. Glucose uptake

Extracellular glucose can be transported directly into the cell by an active transport system followed by intracellular phosphorylation via glucokinase to produce glucose-6-phosphate, but may also be

catabolised by an oxidative periplasmic pathway in which glucose is oxidised via a periplasmic $NAD(P)^+$-independent glucose dehydrogenase (Whitfield et al., 1982). This enzyme uses pyrroloquinoline quinone (PQQ) as cofactor (Goosen et al., 1987; Duine and Jongejan, 1989) and produces gluconate, which is transported into the cell by an active transport system involving gluconate permease. The gluconate is then phosphorylated by an ATP-dependant gluconokinase reaction. The PQQ re-oxidation takes place at the membrane quinone of the respiratory chain and can, therefore, be considered to be equivalent to $FADH_2$ re-oxidation from an energetic viewpoint. Both pathways can function simultaneously though the direct oxidative pathway is normally considered to be operative under conditions of non-constrained glucose availability. In fermentation experiments, a transitory accumulation of gluconate in the extracellular culture media was observed during the culture ($[\text{gluconate}]_{max} = 0.5$ g l^{-1}), indicating that a non quantified fraction of the extracellular glucose was being oxidised to gluconate in the periplasm prior to transport into the cytosol. The extent of this carbon partitioning has never been quantitatively established.

3.2.2. Central metabolic pathways

X. campestris lacks phosphofructokinase activity essential for a functional glycolysis and metabolises glucose via a central cycle which includes the Entner–Doudoroff pathway, as described for *P. aeruginosa* (Hochster and Katznelson, 1958; Temple et al., 1998). Moreover, one of the products of the Entner–Doudoroff pathway, GAP can theoretically be recycled through the central cycle by the way of fructose-1,6-bisphosphate aldolase and fructose-1,6-bisphohatase, rather than being oxidised to pyruvate via the lower part of glycolysis (Hochster and Katznelson, 1958). As for glucose uptake, no reliable quantitative data exists as to the carbon flux distribution at the level of GAP, or the manner in which this may influence the yield of xanthan gum.

3.2.3. Pentose–phosphate pathway

Radio-respirometric studies (Zagallo and Wang, 1967) have indicated that only a small proportion of glucose flux (between 8 and 16%) is routed into the pentose–phosphate pathway under conditions of xanthan production on glucose. This pathway would, therefore, not normally be expected to play an important role during the production of xanthan. Nevertheless, the possible influence of this pathway on the xanthan yield has been studied.

3.2.4. Respiratory chain

Whole cells of *X. campestris* contain cytochromes *b*, *c*, aa_3, *o*-type cytochromes and possibly a_1, and therefore, maximum H^+/O values of 6 for the oxidation of endogenous substrate can be expected (Rye et al., 1988). These data suggest the presence of three sites of proton translocation within the respiratory chain. However, by analogy with the respiratory chain of *Pseudomonas* sp. (Matsushita et al., 1980; Zannoni, 1989), the respiratory chain of *X. campestris* could potentially be branched and electron flux into the different branches of the chain would lead to different energetic efficiencies. If the distribution of electrons into the different branches is taken into consideration, the number of proton translocation sites could vary from two to three for the regeneration of reduced coenzymes such as $NADH,H^+$. If it is then considered that the ATPase reaction is of fixed stoichiometry with 3 H^+ per ATP, then the P^+/O ratio will fall between 1.33 and 2 ATP per $NADH,H^+$ re-oxidised. $FADH_2$ and $PQQH_2$ oxidation are generally considered to involve one less site of proton translocation than $NADH,H^+$ and will, therefore, yield a P^+/O ratio of between 0.67 and 1.33. It has been assumed that the transformation of $NADPH,H^+$ to $NADH,H^+$ does not lead to energy production and that the reverse reaction does not occur, i.e. the $NADPH,H^+$ produced by catabolism was at least equal to the anabolic requirement.

3.3. Maximal yield of xanthan gum

The metabolic network of *X. campestris* is particularly complex and little reliable data exists as to how carbon flux is distributed between the various pathways. Hypothetical carbon flux dis-

tribution and associated yields of xanthan gum were calculated for a number of network configurations representative of possible flux patterns. Initially, sensitivity of the network configuration was examined for carbon distribution at specific network branch points. All calculations were performed with a number of experimental inputs as regards specific rates of growth ($\mu = 0.05\ h^{-1}$) and glucose consumption (2 mmol $g^{-1}\ h^{-1}$) and the previously determined (see above) maintenance coefficient ($m = 0.33$ mmol $g^{-1}\ h^{-1}$).

3.3.1. Influence of the pentose–phosphate pathway

The maximal yield of xanthan gum, containing 0.5 mol of pyruvate and 1 mol of acetate, was first calculated as function of the proportion of 6PG oriented toward the pentose–phosphate pathway and the number of proton translocation sites, assuming that GAP is not recycled towards the central cycle. The glucose was considered to be taken up entirely by the phosphorylative pathway, i.e. no flux through the periplasmic pathway. In this configuration of the metabolic network, xanthan gum production is limited exclusively by the availability of metabolic energy, and the yield of xanthan is not surprisingly dependent on the efficiency of the respiratory chain (Fig. 3A).

The experimental yield of xanthan gum is equal to 0.59 Cmol $Cmol^{-1}$. This yield could be explained whatever the flux of 6PG orientated towards the pentose–phosphate pathway. Thus, the partition of 6PG between Entner–Doudoroff and the pentose–phosphate pathway is not a factor susceptible to modify xanthan gum production yields. In light of this, the flux into the pentose–phosphate pathway was maintained in following configurations at the minimal level necessary to satisfy anabolic precursor requirements. Furthermore, this is in agreement with previous reports indicating a low flux through the pentose–phosphate pathway in *X. campestris* (Zagallo and Wang, 1967).

3.3.2. Influence of the periplasmic oxidative pathway

The maximal yield of xanthan gum was calculated as function of the proportion of extracellular glucose metabolised via the oxidative periplasmic pathway (gluconate bypass) and the number of translocation sites of protons, assuming that GAP was not recycled toward the central cycle. Two

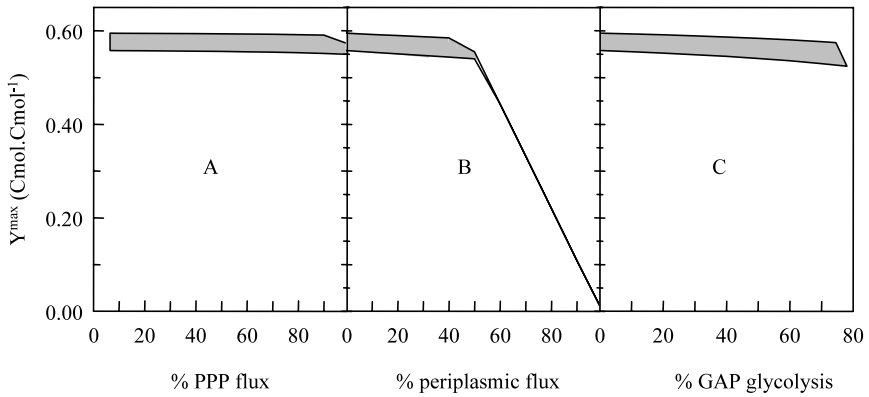

Fig. 3. Influence of different metabolic network configurations and the number of proton translocation sites (two or three) on the maximum theoretical yield of xanthan gum ($Y^{max}_{Xth/S}$) with *X. campestris*. The zone shaded in grey represents the difference between the energetic efficiency of the respiratory chain, i.e. the presence of two or three sites of proton translocation. Theoretical maximum yields were calculated, using inputs of growth rate, sugar consumption and maintenance energy representative of real experimental values. The following configurations were examined: (A) influence of carbon distribution between the pentose–phosphate pathway and the Entner–Doudoroff pathway; (B) carbon distribution between the periplasmic oxidative pathway and the cytosolic phosphorylative pathway; and (C) carbon distribution at the level of GAP between glycolysis (GAP dehydrogenase) and the hexose cycle (fructose-1,6-bisphosphate aldolase).

metabolic situations can be identified as a function of the flux distribution (Fig. 3B). If the glucose is transported into the cell predominantly after transformation to gluconate via the oxidative periplasmic pathway, xanthan gum production would be limited by carbon availability due to the network structure. Indeed, if all glucose enters the cytosol via the gluconate by-pass, no synthesis of xanthan gum can occur. On the other hand, if a majority of glucose enters the cell via the phosphorylative pathway, xanthan gum formation is limited by the availability of biochemical energy. The experimental data are in good agreement with this second model of cellular metabolism and suggest, therefore, that only a relatively small amount of glucose is oxidised via the periplasmic pathway under the fermentation conditions employed here. However, it should be noted that any significant increase in flux towards gluconate might be expected to decrease experimental yields of xanthan.

3.3.3. *Influence of the recycling of GAP*

Fructose-1,6-bisphophatase, fructose-1,6-bisphosphate aldolase and GAP dehydrogenase activities were all shown to be present throughout the culture. Furthermore, the specific activities of these three enzymes remained constant at all times with specific activities of 70, 20 and 550 nmol mg^{-1} protein min^{-1}, respectively. From these values it is difficult to predict how carbon flux at the level of GAP will be determined and the possible metabolic configurations need to be analysed. The consequences of a variable proportion of GAP recycling towards the central cycle (gluconeogenesis) was examined to see how this might affect the xanthan yield. As previously stated, it was assumed that the flux into the pentose–phosphate pathway was diminished to the minimum required for anabolic precursor synthesis and that the extracellular glucose enters the network exclusively via the phosphorylative pathway. In this network structure, xanthan gum production is also exclusively limited by energy availability and consequently maximal xanthan yields are governed by the efficiency of the respiratory chain (Fig. 3C). As the proportion of GAP recycled to the central cycle is increased, the theoretical xanthan yield can be seen to diminish slightly. This is due to the difference of energetic efficiency between glycolysis and the gluconeogenic pathway. Orientation of GAP towards glycolysis leads to higher energy generation and increases, therefore, the maximal yield of xanthan. Flux recycling, while likely to increase availability of glucose-6-phosphate and fructose-6-phosphate for the xanthan biosynthetic pathways leads to an increased energy consumption at the level of fructose-1,6-biphosphatase, accentuating the energetic limitation due to the diminished flux into energy-generation glycolysis. However, this variation is of only minor importance for network configurations in which direct uptake and phosphorylation of glucose occurs.

3.3.4. *Determination of the maximal yield of xanthan*

Each of the above network configurations is a rather extreme case in which only a single branch-point has been varied. In light of this, a second approach has been used. The theoretical yield of xanthan has been calculated as a function of the proportion of the extracellular glucose flux passing via the oxidative periplasmic pathway and the number of proton translocation sites, without imposing further constraints on the recycling of GAP. The pentose–phosphate pathway was maintained at the minimal level, but variation of flux at this level effectively provokes a similar effect on xanthan yield as GAP recycling (results not shown). Unlike the previous simulation (Fig. 3) examining the effect of glucose distribution on xanthan yield, a somewhat modified prediction was observed (Fig. 4). When extracellular glucose was orientated towards periplasmic oxidation prior to uptake at the level of gluconate, the xanthan yield can be seen to be carbon limited though to a considerably lower extent than previously. Under such conditions, metabolism would generate energy in excess, facilitating the energetically unfavourable orientation of GAP towards the central cycle, with only a minimal flux for precursor synthesis through GAP dehydrogenase. As previously determined, a flux passing predominantly via glucose uptake and phosphorylation leads to the yield of xanthan

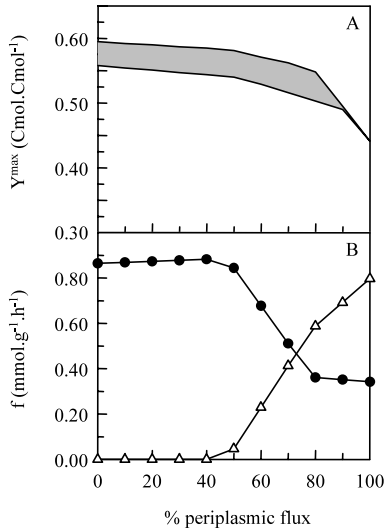

Fig. 4. Effect of flux partitioning between the periplasmic oxidative pathway and the phosphorylative pathway of glucose metabolism on maximal xanthan yields and flux partitioning elsewhere in the network. (A) Maximal theoretical yield of xanthan ($Y^{max}_{Xth/S}$) as a function of the flux distribution between the oxidative and the phosphorylative pathway of glucose catabolism with unconstrained flux partitioning at the level of GAP. The zone shaded in grey represents the difference between the energetic efficiency of the respiratory chain, i.e. the presence of two or three sites of proton translocation. (B) flux distribution predicted at the level of GAP metabolism through fructose-1,6-bisphosphate aldolase (△) and GAP dehydrogenase (●) in order to attain maximal theoretical xanthan yields.

gum being energy limited. Under such conditions, the flux recycling of GAP towards the central cycle is diminished in order to produce the energy necessary for maximal biosynthesis of xanthan gum. Thus, the intensity of the flux through fructose-1,6-bisphophate aldolase would decrease as a function of the proportion of glucose uptake and phosphorylation, reaching zero (i.e. all flux orientated through GAP dehydrogenase) when the uptake of glucose exceeded 60% of total glucose consumption (Fig. 4). The maximal yield of xanthan gum diminished with the proportion of the extracellular glucose orientated into the oxidative periplasmic pathway due to the difference between the energetic yield of the re-oxidation of PQQ and NAD(P)H,H^+.

3.4. Dynamic evolution of the metabolic constraints throughout the culture

The above constraint modelling used specific rates representative of a single data point within a fermentation, but both growth and glucose consumption rates changed throughout the culture. The theoretical maximal yield of xanthan gum was, therefore, calculated at five points representative of the dynamic evolution of kinetic parameters throughout the cultivation period (Table 2) and compared with experimental yields. Changes in chemical composition of xanthan, previously shown to be important when sucrose was used as feedstock (Letisse et al., 2001), were greatly attenuated on glucose though some increase in acetate substitution at the expense of pyruvate was observed. This did not provoke any significant variation in the overall yield predictions, however. The estimated maximal yield potential for xanthan gum was, therefore, determined as a function of the proportion of extracellular glucose flux passing into the oxidative pathway and the number of proton translocation sites, without imposing constraints on the recycling of GAP.

The maximal theoretical yield of xanthan gum, based upon kinetic inputs concerning sugar uptake and growth rates increased throughout the culture as observed for experimental yields. This was mainly due to the decreased energy demand resulting from the diminished growth rate (Table 2), but also to the increased carbon metabolite availability since anabolic precursor metabolites were not removed from the network. As might be logically predicted from this shift from biomass synthesis to xanthan production, the sensitivity of the network structure to carbon limitation constraints was progressively diminished. It is, therefore, unlikely that variations in the flux through the central pathways will have a significant effect on xanthan yields during the latter part of the culture. It is interesting to observe that the predicted yields are in good agreement with the observed experimental yields. Energy availability is clearly the dominant constraint on xanthan gum production except under hypothetical configurations in which the direct oxidative pathway is responsible for virtually all consumption of glu-

Table 2
Experimental values of kinetic data throughout the culture on glucose

Time (h)	μ	q_s	$Y^{exp}_{Xth/S}$	Metabolic constraints	
				Periplasmic flux (%)	GAP recycling (%)
22.5	0.07	2.36	0.55	50–20 (100–50)	11–74 (0)
30	0.05	2.00	0.57	100–20 (100–40)	0–77 (0–31)
40	0.03	1.54	0.56	100–20 (100–40)	0–77 (0–28)
50	0.01	1.21	0.62	100–20 (100–50)	0–83 (0–12)
60	0	1.05	0.65	100–20 (100–50)	0–88 (0–21)

The metabolic constraints are the extent to which the flux through specific biochemical pathways can be varied while retaining theoretical xanthan yields (Cmol Cmol^{-1}) coherent with observed experimental yields ($Y^{exp}_{Xth/S}$). Values given are for a respiratory chain possessing three sites of proton translocation, while values in brackets are those values which are imposed when only two sites of proton translocation are considered.

cose. Since such a situation leads to yields which fall below those observed experimentally, it can be assumed that such a situation was not functioning under the operating conditions employed in this study. However, as much as 80% of sugar could theoretically pass via this periplasmic pathway without adversely modifying the yield prediction, though such values require compensatory flux modifications so as to avoid carbon limitation, notably as regards recycling of metabolites towards the xanthan biosynthetic pathways via the hexose cycle. Since energy production is rather difficult to modify, any increased carbon flux towards the more energetically favourable pathways will lead rapidly to carbon limitations, future research should attempt to see whether the rather high energy requirement for maintenance is representative of real biochemical energy-requiring processes, or can be some extent attributed to energy spilling reactions (futile cycles) which artificially increase the apparent maintenance requirements. If futile cycles can be identified, genetic engineering strategies susceptible to increase product yields can be envisaged. Otherwise, it would appear that product yields are now close to those attainable without major restructuring of the metabolic pathways of *X. campestris* and further increases in performance will concern productivity and product quality.

References

Ampe, F., de Aragao, G.M.F., Uribelarrea, J.L., Lindley, N.D., 1997. Benzoate degradation via the ortho pathway in *Alcaligenes eutrophus* is perturbed by succinate. Appl. Environ. Microbiol. 63, 2765–2770.

Becker, A., Katzen, F., Pühler, A., Ielpi, L., 1998. Xanthan gum biosynthesis and application: a biochemical/genetic perspective. Appl. Microbiol. Biotechnol. 50, 145–152.

Conrad, R., Schlegel, H.G., 1977. Different degradation pathways for glucose and fructose in *Rhodopseudomonas capsulata*. Arch. Microbiol. 112, 39–48.

Dominguez, H., Rollin, C., Guyonvarch, A., Guerquin-Kern, J.-L., Cocaign-Bousquet, M., Lindley, N.D., 1998. Carbon flux distribution in the central metabolic pathways of *Corynebacterium glutamicum* during growth on fructose. Eur. J. Biochem. 254, 96–102.

Duine, J.A., Jongejan, J.A., 1989. Quinoproteins, enzymes with pyrrolo–quinoline quinone as cofactor. Ann. Rev. Biochem. 58, 403–426.

Goosen, N., Vermasas, D.A.M., Van de Putte, P., 1987. Cloning of the genes involved in synthesis of coenzyme pyrrolo–quinoline–quinone from *Acetinobacter calcoaceticus*. J. Bacteriol. 169, 303–646.

Hochster, R.M., Katznelson, H., 1958. On the mechanism of glucose-6-phosphate oxidation in cell-free extracts of *Xanthomonas phaseoli*. Can. J. Biochem. Physiol. 36, 669–689.

Jarman, T.R., Pace, G.W., 1984. Energy requirement for microbial exopolysaccharide synthesis. Arch. Microbiol. 137, 231–235.

Letisse, F.P., Chevallereau, P., Simon, J.-L., Lindley, N.D., 2001. Kinetic analysis of xanthan gum production with *Xanthomonas campestris* on sucrose using sequentially

consumed nitrogen sources. Appl. Microbiol. Biotechnol. 55, 417–422.

Loubiere, P., Gros, E., Paquet, V., Lindley, N.D., 1992. Kinetics and physiological implications of the growth behaviour of *Eubacterium limosum* on glucose/methanol mixtures. J. Gen. Microbiol. 138, 979–985.

Matsushita, K., Yamada, M., Shinagawa, E., Adachi, O., Ameyama, M., 1980. Membrane bound respiratory chain of *Pseudomonas aeruginosa* grown aerobically. J. Bacteriol. 141, 389–392.

Rye, A.J., Drozd, J.W., Jones, C.W., Linton, J.D., 1988. Growth efficiency of *Xanthomonas campestris* in continuous culture. J. Gen. Microbiol. 134, 1055–1061.

Temple, L.M., Sage, A.E., Schweizer, H.P., Phibbs, P.V., 1998. Carbohydrate catabolism in *Pseudomonas aeruginosa*. In: Montie, T.C. (Ed.), Pseudomonas. Plenum Press, New York and London, pp. 35–72.

Whitfield, C., Sutherland, I.W., Cripps, R.E., 1982. Glucose metabolism in *Xanthomonas campestris*. J. Gen. Microbiol. 128, 981–985.

Zagallo, A.C., Wang, C.H., 1967. Comparative glucose catabolism of *Xanthomonas* species. J. Bacteriol. 93, 970–975.

Zannoni, D., 1989. The respiratory chain of pathogenic pseudomonads. Biochim. Biophys. Acta 975, 299–316.